

# Rethinking the Implementation Tricks and Monotonicity Constraint in Cooperative Multi-Agent Reinforcement Learning

**Jian Hu** <sup>\*</sup>

Graduate Institute of Networking and Multimedia  
National Taiwan University  
Taipei  
r08944053@ntu.edu.tw

**Siyang Jiang** <sup>\*</sup>

Graduate Institute of Electrical Engineering  
National Taiwan University  
Taipei  
syjiang@arbor.ee.ntu.edu.tw

**Seth Austin Harding**

Department of Computer Science  
National Taiwan University  
Taipei  
b06902101@ntu.edu.tw

**Haibin Wu**

Graduate Institute of Communication Engineering  
National Taiwan University  
Taipei  
f07921092@ntu.edu.tw

**Shih-wei Liao**

Department of Computer Science  
National Taiwan University  
Taipei  
liao@csie.ntu.edu.tw

**Abstract:** Many complex multi-robot systems such as robot swarms control and autonomous vehicle coordination can be modeled as Multi-Agent Reinforcement Learning (MARL) tasks. QMIX, a widely popular MARL algorithm, has been used as a baseline for the benchmark environments, e.g., Starcraft Multi-Agent Challenge (SMAC), Difficulty-Enhanced Predator-Prey (DEPP). Recent variants of QMIX target relaxing the monotonicity constraint of QMIX, allowing for performance improvement in SMAC. In this paper, we investigate the code-level optimizations of these variants and the monotonicity constraint. (1) We find that such improvements of the variants are significantly affected by various code-level optimizations. (2) The experiment results show that QMIX with normalized optimizations outperforms other works in SMAC; (3) beyond the common wisdom from these works, the monotonicity constraint can improve sample efficiency in SMAC and DEPP. We also discuss why monotonicity constraints work well in purely cooperative tasks with a theoretical analysis. We open-source the code at <https://github.com/hijkzzz/pymarl2>.

**Keywords:** Multi-Agent, Reinforcement Learning, Monotonicity Constraint

## 1 Introduction

As more robots are deployed in various scenarios, such as robot swarm control [1, 2, 3], autonomous vehicle coordination [4, 5], and sensor networks [6], a complex task always requires multi-robot to accomplish together. Multi-Robot Reinforcement Learning (MRRL), or generally named Multi-Agent Reinforcement Learning (MARL), is used to solve the multi-robot systems tasks [2].

In multi-robot systems, a typical challenge is a limited scalability and inherent constraints on agent observability and communication. Therefore, decentralized policies that act only on their local

<sup>\*</sup>Jian Hu and Siyang Jiang contributed equally to this work.

<sup>†</sup>Corresponding author.

observations are necessitated and widely used [7]. Learning decentralized policies is an intuitive approach for training agents independently. However, simultaneous exploration by multiple agents often results in non-stationary environments, which leads to unstable learning. Therefore, *Centralized Training and Decentralized Execution* (CTDE) [8] allows for independent agents to access additional state information that is unavailable during policy inference.

Another challenge in cooperative multi-robot systems is the lacking of real samples, such as samples from crash drones or autonomous vehicles [5]. Therefore, many CTDE learning algorithms have been proposed for the better sample efficiency in cooperative tasks[9]. Among them, several value-based approaches achieve state-of-the-art (SOTA) performance [10, 11, 12, 13] on such benchmark environments, e.g., Starcraft Multi-Agent Challenge (SMAC) [14], Difficulty-Enhanced Predator-Prey (DEPP) [15, 16]. To enable effective CTDE for multi-agent Q-learning, the Individual-Global-Max (IGM) principle [17] of equivalence of joint greedy action and individual greedy actions is critical. The primary advantage of the IGM principle is that it ensures consistency of policy with centralized training and decentralized execution. To ensure IGM principle, QMIX [10] was proposed for factorizing the joint action-value function with the *Monotonicity Constraint* [11], however, limiting the expressive power of the mixing network.

To generalize and improve the performance of QMIX, some variants of QMIX<sup>3</sup>, including value-based approaches [12, 13, 11, 18] and a policy-based approach [7], have been proposed with the aim to relax the monotonicity constraint of QMIX. However, while investigating the codes of these variants, we find that their performance is significantly affected by their code-level optimizations (or implementation tricks). Therefore, it is left unclear whether monotonicity constraint indeed impairs the QMIX’s performance.

In this paper, we investigate the impact of the *code-level optimizations* and the *monotonicity constraint* in cooperative MARL. Firstly, we investigate the effects of code-level optimizations, which enable QMIX to solve the most difficult challenges in SMAC. Afterward, we normalize the optimizations of QMIX and its variants; specifically, we perform the same hyperparameter search pattern for all algorithms, which includes using or removing a certain optimization and a grid hyperparameter search; the experiment results (Sec. 5.2.1) demonstrate that QMIX outperforms the other variants. Secondly, to study the impact of the monotonicity constraint, we propose a policy-based algorithm, RIIT; the experimental results (Sec. 5.2.2) show that the monotonicity constraint improves sample efficiency in SMAC and DEPP. Lastly, to generalize cooperative tasks beyond SMAC and DEPP, we give a strict definition of purely cooperative tasks and a discussion about why monotonicity constraints work well in purely cooperative tasks.

To our best knowledge, this work is the first to analyze the monotonicity constraint and code-level optimizations in MARL. Our broader impact for multi-robot learning is demonstrated in Section 8.

## 2 Preliminaries

**Dec-POMDP.** We model the multi-robot RL problem as decentralized partially observable Markov decision process (Dec-POMDP) [19], which composed of a tuple  $G = \langle \mathcal{S}, \mathcal{U}, P, r, \mathcal{Z}, O, N, \gamma \rangle$ .  $s \in \mathcal{S}$  describes the true state of the environment. At each time step, each agent  $i \in \mathcal{N} := \{1, \dots, N\}$  chooses an action  $u^i \in \mathcal{U}$ , forming a joint action  $\mathbf{u} \in \mathcal{U}^N$ . All state transition dynamics are defined by function  $P(s' | s, \mathbf{u}) : \mathcal{S} \times \mathcal{U}^N \times \mathcal{S} \mapsto [0, 1]$ . Each agent has independent observation  $z \in \mathcal{Z}$ , determined by observation function  $O(s, i) : \mathcal{S} \times \mathcal{N} \mapsto \mathcal{Z}$ . All agents share the same reward function  $r(s, \mathbf{u}) : \mathcal{S} \times \mathcal{U}^N \rightarrow \mathbb{R}$  and  $\gamma \in [0, 1)$  is the discount factor. The objective function, shown in Eq. 1, is to maximize the joint value function to find a joint policy  $\pi = \langle \pi_1, \dots, \pi_n \rangle$ .

$$J(\pi) = \mathbb{E}_{u^1 \sim \pi^1, \dots, u^N \sim \pi^N, s \sim T} \left[ \sum_{t=0}^{\infty} \gamma^t r_t(s_t, u_t^1, \dots, u_t^N) \right] \quad (1)$$

**Centralized Training and Decentralized Execution (CTDE).** CTDE is a popular paradigm [11] which allows for the learning process to utilize additional state information [8]. Agents are trained in a centralized way, i.e., learning algorithms, to access all local action observation histograms, global states, and sharing gradients and parameters. In the execution stage, each individual agent can only access its local action observation history  $\tau^i$ .

<sup>3</sup>These algorithms are based on the mixing network from QMIX, so we call the variants of QMIX.

**QMIX and Monotonicity Constraint.** To resolve the credit assignment problem in multi-agent learning, QMIX [10] learns a joint action-value function  $Q_{tot}$  which can be represented in Eq. 2:

$$Q_{tot}(s, \mathbf{u}; \boldsymbol{\theta}, \phi) = g_\phi(s, Q_1(\tau^1, u^1; \theta^1), \dots, Q_N(\tau^N, u^N; \theta^N))$$

$$\frac{\partial Q_{tot}(s, \mathbf{u}; \boldsymbol{\theta}, \phi)}{\partial Q_i(\tau^i, u^i; \theta^i)} \geq 0, \quad \forall i \in \mathcal{N} \quad (2)$$

where  $\phi$  is the trainable parameter of the monotonic mixing network, which is a mixing network with monotonicity constraint, and  $\theta^i$  is the parameter of the agent network  $i$ . Benefiting from the monotonicity constraint in Eq. 2, maximizing joint  $Q_{tot}$  is precisely the equivalent of maximizing individual  $Q_i$ , resulting in and allowing for optimal individual action to maintain consistency with optimal joint action. QMIX learns by sampling a multitude of transitions from the replay buffer and minimizing the mean squared temporal-difference (TD) error loss:

$$\mathcal{L}(\theta) = \frac{1}{2} \sum_{i=1}^b \left[ (y_i - Q_{tot}(s, u; \theta, \phi))^2 \right] \quad (3)$$

where the TD target value  $y = r + \gamma \max_{u'} Q_{tot}(s', u'; \theta^-, \phi^-)$  and  $\theta^-, \phi^-$  are the target network parameters copied periodically from the current network and kept constant for a number of iterations. However, the monotonicity constraint limits the mixing network’s expressiveness, which may fail to

<b>12</b>	-12	-12
-12	<b>0</b>	<b>0</b>
-12	0	0

(a) Payoff matrix

-12	-12	-12
-12	<b>0</b>	<b>0</b>
-12	0	0

(b) QMIX:  $Q_{tot}$

Table 1: A non-monotonic matrix game. Bold text indicates the reward of the argmax action.

learn in non-monotonic cases [20] [13]. Table 1a shows a non-monotonic matrix game that violates the monotonicity constraint. This game requires both robots to select the first action 0 (actions are indexed from top to bottom, left to right) in order to catch the reward 12; if only one robot selects action 0, the reward is -12. QMIX may learn an incorrect  $Q_{tot}$  which has an incorrect argmax action as shown in Table 1b.

### 3 Related Works

In this section, we describe the variants of QMIX and investigate various code-level optimization works. We explain the details of these algorithms and show the code resources in Appendix F.

**Value-based Methods** To enhance the expressive power of QMIX, Qatten [12] introduces an attention mechanism to enhance the expression of QMIX; QPLEX [11] transfers the monotonicity constraint from Q values to Advantage values [21]; QTRAN++ [18] and WQMIX [13] further relax the monotonicity constraint through a true value network and some theoretical constraints; however, Value-Decomposition Networks (VDNs) [22] only requires a linear decomposition where  $Q_{tot} = \sum_i^N Q_i$ , which can be seen as strengthening the monotonicity constraint.

**Policy-based Methods** LICA [7] completely removes the monotonicity constraint through a policy mixing critic. For other MARL policy-based methods, VMIX [23] combines the Advantage Actor-Critic (A2C) [24] with QMIX to extend the monotonicity constraint to value networks, i.e., replacing the value network with the monotonic mixing network. DOP [25] learns the policy networks using the Counterfactual Multi-Agent Policy Gradients (COMA) [26] with the  $Q_i$  decomposed by QMIX.

### 4 Experiments Setup

To facilitate the study of cooperation in complex multi-robots scenarios,, we simulate the interaction among the robots through two hard computer games.

## 4.1 Benchmark Environment

**StarCraft Multi-Agent Challenge (SMAC)** is used as our main benchmark testing environment, which is a ubiquitously-used multi-agent cooperative control environment for MARL algorithms [11, 10, 18, 13]. SMAC consists of a set of StarCraft II micro battle scenarios, whose goals are for allied robots to defeat enemy robots, and it classifies micro scenarios into *Easy*, *Hard*, and *Super Hard* levels. The simplest VDNs [22] can effectively solve the Easy scenarios. It is worth noting that QMIX and VDNs achieves a 0% win rate in three Super Hard scenarios *corridor*, *3s5z\_vs\_3s5z*, and *6h\_vs\_8z* [14]. Therefore, we mainly investigate the Hard and Super Hard scenarios in SMAC.

**Difficulty-Enhanced Predator-Prey (DEPP)** In vanilla Predator-Prey (PP) [27], three cooperating agents control three robot predators to chase a faster robot prey (the prey acts randomly). The goal is to capture the prey with the fewest steps possible. We leverage two difficulty-enhanced Predator-Prey variants to test the algorithms: (1) the first variant of Predator-Prey [15] requires two predators to catch the prey at the same time to get a reward; (2) In the Continuous Predator-Prey [16], the prey’s policy is replaced by a hard-coded heuristic, seeing details in Appendix C.

## 4.2 Evaluation Metric

Our primary evaluation metric is the function that maps the steps for the environment observed throughout the training to the median winning percentage (episode return for Predator-Prey) of the evaluation. Just as in QMIX [10], we repeat each experiment with several independent training runs (five independent random experiments). To accurately evaluate the convergence performance of each algorithm, eight rollout processes for parallel sampling are used to obtain as many samples as possible from the environments at a high rate. Specifically, our experiments can collect 10 million samples within 9 hours with a Core i7-7820X CPU and a GTX 1080 Ti GPU.

## 5 Experiments

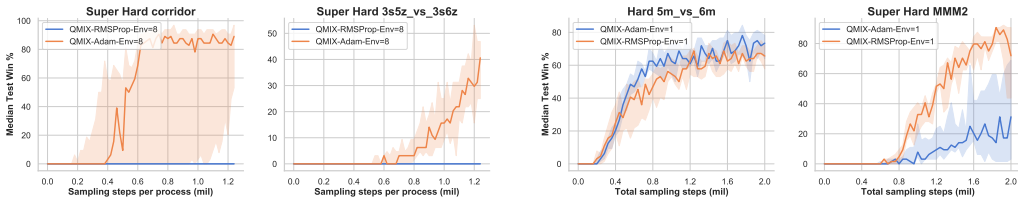
Our experiments consist of two parts. The first part demonstrates the performance of several isolated tricks from the variants. The second part is the reconceptualization of the monotonicity constraint.

### 5.1 Rethinking the Code-level Optimizations

The code-level optimizations are the tricks unaccounted for in the experimental design, but that might hold significant effects on the result. To better understand their influences on performance, we perform ablation experiments on these tricks incrementally and provide some suggestions for tuning. We study the major optimizations here, and introduce the other tricks in Appendix A.

#### 5.1.1 Optimizer

**Study description.** QMIX and the majority of its variant algorithms use RMSProp to optimize neural networks as they prove stable in SMAC. We attempt to use Adam to optimize QMIX’s neural network with quickly convergence benefiting from momentum:



(a) Eight rollout processes are used for sampling.

(b) Only one rollout process is used for sampling.

Figure 1: (a) Adam significantly improves performance when samples are updated quickly; (b) The Q networks optimized by Adam is prone to overfitting when samples are updated slowly.

**Interpretation.** Figure 1a shows that Adam [28] increases the win rate by 100% on the Super Hard map *corridor*. Adam boosts the network’s convergence allowing for full utilization of the large

quantity of samples sampled in parallel. However, Figure 1b shows that when we use only one sampling process, samples are updated slower than with eight processes (the replay buffer size is fixed), and the neural network becomes prone to overfitting. We find that the Adam optimizer solves the problem posed by [23] in which QMIX does not work well under parallel training.

**Recommendation.** Use Adam and quickly update the samples; or reducing the learning rate when the samples update slowly.

### 5.1.2 Eligibility Traces

**Study description.** Eligibility traces such as  $TD(\lambda)$  [29], Peng’s  $Q(\lambda)$  [30], and  $TB(\lambda)$  [31] achieve a balance between return-based algorithms (where return refers to the sum of discounted rewards  $\sum_t \gamma^t r_t$ ) and bootstrap algorithms (where return refers to  $r_t + V(s_{t+1})$ ), speeding up the convergence of reinforcement learning algorithms. Therefore, we study the application of Peng’s  $Q(\lambda)$ .

**Interpretation.** Q networks without sufficient training usually have a large bias that impacts bootstrap returns. Figure 2a shows that  $Q(\lambda)$  allows for faster convergence in our experiments by reducing this bias. However, large values of  $\lambda$  may lead to failed convergence due to variance and off-policy bias. Figure 2a shows that when  $\lambda$  is set to 0.9, it has a detrimental impact on the performance of QMIX.

**Recommendation.** Use  $Q(\lambda)$  with a small value of  $\lambda$ .

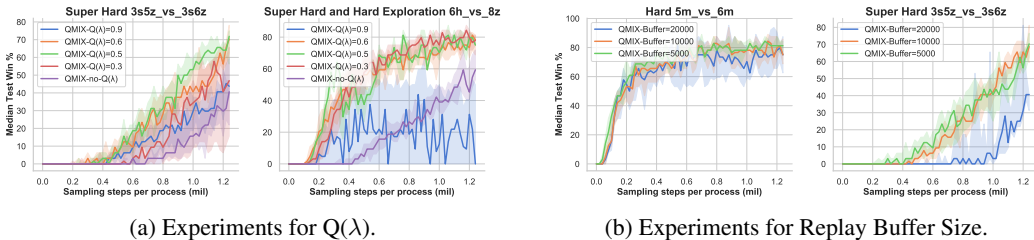


Figure 2: (a)  $Q(\lambda)$  significantly improves performance of QMIX, but large values of  $\lambda$  lead to instability in the algorithm. (b) Setting the replay buffer size to 5000 episodes allows for QMIX’s learning to be more stable than by setting it to 20000 episodes.

### 5.1.3 Replay Buffer Size

**Study description.** In single-agent Deep Q-networks (DQN), the replay buffer size is usually set to a large value. However, in multi-agent tasks, as the action space becomes larger than that of single-agent tasks, the distribution of samples changes more quickly. In this section, we study the impact of the replay buffer size on performance.

**Interpretation.** Figure 2b shows that a large replay buffer size causes instability in QMIX’s learning. The causes of this phenomenon are as follows: (1) In multi-agent tasks, samples become obsolete more quickly than in single-agent tasks. (2) Echoing in Sec. 5.1.1, Adam performs better with samples with fast updates. (3) When the sampling policy is far from the current policy, the return-based methods require importance sampling ratios, which is difficult to calculate in multi-agent learning.

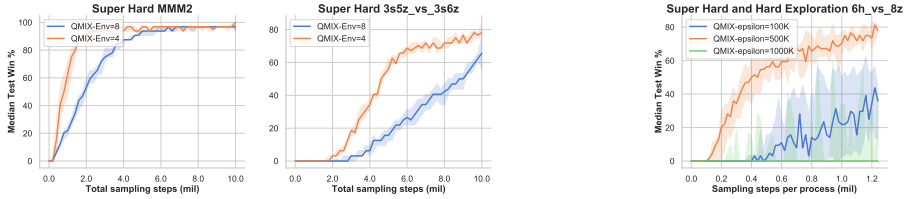
**Recommendation.** Use a small replay buffer size.

### 5.1.4 Rollout Process Number

**Study description.** When we collect samples in parallel as is done in A2C [24], it shows that when there is a defined total number of samples and an unspecified number of rollout processes, the median test performance becomes inconsistent. This study aims to perform analysis and provide insight on the impact of the number of processes on the final performance.

**Interpretation.** Under the A2C [21] training paradigm, the total number of samples can be calculated as  $S = E \cdot P \cdot I$ , where S is the total number of samples, E is the number of samples in each episode, P is the number of rollout processes, and I is the number of policy iterations. Figure 3a shows that we are given both S and E; the fewer the number of rollout processes, the greater the number of policy iterations [29]; a higher number of policy iterations leads to an increase in performance. However, it also causes both longer training time and decreased stability.

**Recommendation.** Use fewer rollout processes when samples are difficult to obtain, especially for real-world robot learning; otherwise, use more rollout processes.



(a) Experiments for Rollout Process Number.

(b) Experiments for  $\epsilon$  anneal period.

Figure 3: (a) Given the total number of samples, fewer processes achieve better performance. We set the replay buffer size to be proportional to the number of processes to ensure that the novelty of the samples is consistent. (b) On the hard-to-explore scenario  $6h\_vs\_8z$ , defining a proper length for  $\epsilon$  anneal period significantly improves performance.

### 5.1.5 Exploration Steps

**Study description.** Some scenarios in SMAC are hard to explore, such as  $6h\_vs\_8z$ , so the settings of  $\epsilon$ -greedy become critically important. In this study, we analyze the effect of  $\epsilon$  anneal period on performance.

**Interpretation.** As shown in Figure 3b, increasing the length of the  $\epsilon$  anneal period from 100K steps to 500K steps allows for a 38% increase in win rate in the Super Hard Exploration scenario  $6h\_vs\_8z$ . However, increasing this value to 1000K instead causes the model to collapse.

**Recommendation.** Increase the value of the  $\epsilon$  anneal period to an appropriate length on hard-to-explore scenarios.

## 5.2 Rethinking the Monotonicity Constraint

In this subsection, we investigate the overall impact of above optimizations. Then, we normalize the optimizations for all algorithms, i.e., the same hyperparameter search pattern is used for all algorithms, which includes whether we use a certain optimization as well as a grid search for these hyperparameters (details in Appendix D). We denote the optimized algorithms with the prefix *Our*. Second, RIIT and VMIX are demonstrated to further study the effects of the monotonicity constraint.

### 5.2.1 Performance Comparison

Scenarios	Difficulty	QMIX	OurQMIX
2s_vs_1sc	Easy	-	<b>100%</b>
2s3z	Easy	-	<b>100%</b>
1c3s5z	Easy	-	<b>100%</b>
3s5z	Easy	-	<b>100%</b>
10m_vs_11m	Easy	-	<b>100%</b>
8m_vs_9m	Hard	98%	<b>100%</b>
5m_vs_6m	Hard	84%	<b>90%</b>
3s_vs_5z	Hard	96%	<b>100%</b>
bane_vs_bane	Hard	<b>100%</b>	<b>100%</b>
2c_vs_64zg	Hard	<b>100%</b>	<b>100%</b>
corridor	Super Hard	0%	<b>100%</b>
MMM2	Super Hard	98%	<b>100%</b>
3s5z_vs_3s6z	Super Hard	3%	<b>85%</b> (envs = 4)
27m_vs_30m	Super Hard	56%	<b>100%</b>
6h_vs_8z	Super Hard	0%	<b>93%</b> ( $\lambda = 0.3$ )

Table 2: Best median test win rate of OurQMIX and QMIX (batch size=128) in all scenarios.

As shown in Table 2, OurQMIX attains higher win rates in all hard and super hard SMAC scenarios, far exceeding vanilla QMIX. These optimizations are vital for multi-robot reinforcement learning due to high sample efficiency.

Algo.	Type	3s_vs_5z	5m_vs_6m	3s5z_vs_3s6z	corridor	6h_vs_8z	MMM2	PP
OurQMIX	VB	<b>100%</b>	<b>90%</b>	<b>75%</b>	<b>100%</b>	84%	<b>100%</b>	<b>40</b>
OurVDNs	VB	<b>100%</b>	<b>90%</b>	43%	98%	<b>87%</b>	96%	39
OurQatten	VB	<b>100%</b>	<b>90%</b>	62%	<b>100%</b>	68%	<b>100%</b>	-
OurQPLEX	VB	<b>100%</b>	<b>90%</b>	68%	96%	78%	<b>100%</b>	39
OurWQMIX	VB	<b>100%</b>	<b>90%</b>	6%	96%	78%	23%	39
OurLICA	PG	3%	53%	0%	0%	4%	0%	30
OurDOP	PG	0%	9%	0%	0%	1%	0%	32
RIIT	PG	96%	67%	<b>75%</b>	<b>100%</b>	19%	<b>100%</b>	38

Table 3: Median test win rate (episode return) of QMIX-based algorithms with normalized tricks. PG denotes Policy-gradient; VB denotes Value-based; PP denotes Predator-Prey. We compare their performance in the seven most difficult scenarios of SMAC and DEPP.

Next, as shown in Table 3<sup>4</sup>, the test results on the hardest scenarios in SMAC and DEPP demonstrate that **(I)** The performance of *Our* values-based methods exceeds the test results in the past literatures [14, 11, 16, 13] (details in Appendix D.3). **(II)** OurQMIX outperforms other methods. **(III)** The linear OurVDNs is also relatively effective. **(IV)** When the sample size is reduced from 64 million used by LICA [7] to 10 million, LICA has terrible performance. **(V)** The performance of the algorithm becomes progressively worse as the monotonicity constraint decreases (QMIX > QPLEX > WQMIX > LICA, details in Appendix F.8) in the benchmark environment. The experimental results, specifically **(II)**, **(III)**, **(V)**, show that these variants of QMIX that relax the monotonicity constraint do not obtain better performance than QMIX in either SMAC or DEPP.

## 5.2.2 Ablation Studies of Monotonicity Constraint

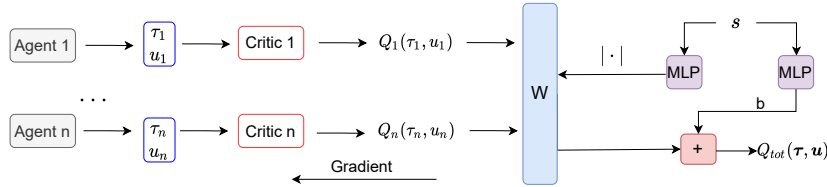


Figure 4: Architecture for RIIT:  $|\cdot|$  denotes absolute value operation, implementing the monotonicity constraint of QMIX.  $W$  denotes the non-negative mixing weights. Agent  $i$  denotes the policy network which can be trained end-to-end by maximizing the  $Q_{tot}$ .

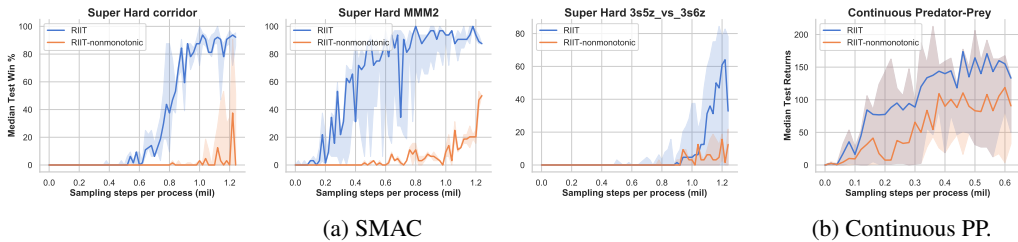


Figure 5: Comparing RIIT w./ and w/o. monotonicity constraint (remove absolute value operation) on SMAC (a) and Continuous Predator-Prey (b).

We further study the impact of monotonicity constraint tasks via comparing the performance of adding or removing the constraint. An end-to-end Actor-Critic method, RIIT, is proposed. Specifically, we use the monotonic mixing network as a critic network, shown in Figure 4. Then, in Eq. 4, with a trained critic  $Q_{\theta_c}^\pi$  estimate, the decentralized policy networks  $\pi_{\theta_i}^i$  can then be optimized end-to-end simultaneously by maximizing  $Q_{\theta_c}^\pi$  with the policies  $\pi_{\theta_i}^i$  as inputs. Since RIIT is trained end-to-end, it may also be used for continuous control tasks. It is worth stating that the item  $\mathbb{E}_i [\mathcal{H}(\pi_{\theta_i}^i(\cdot | z_t^i))]$  is

<sup>4</sup>We avoid using the optimal hyperparameters for QMIX in the comparison, so the experimental results of QMIX in Table 2 are different from those found in Table 3.

the Adaptive Entropy [7], and we use a two-stage approach to train the actor-critic network, described in detail in Appendix E.

$$\max_{\theta} \mathbb{E}_{t, s_t, u_t^1, \dots, \tau_t^n} [Q_{\theta_c}^{\pi} (s_t, \pi_{\theta_1}^1 (\cdot | \tau_t^1), \dots, \pi_{\theta_n}^n (\cdot | \tau_t^n)) + \mathbb{E}_i [\mathcal{H} (\pi_{\theta_i}^i (\cdot | \tau_t^i))]] \quad (4)$$

The monotonicity constraint on the critic (Figure 4) is theoretically no longer required as the critic is not used for greedy action selection. We can evaluate the effects of the monotonicity constraint by removing the absolute value operation in the monotonic mixing network. In this way, RIIT can also be easily extended to non-monotonic tasks. Figure 5a and Figure 5b demonstrate that the monotonicity constraint significantly improves the performance of RIIT. Table 3 also presents that RIIT performs best among the policy-based algorithms.

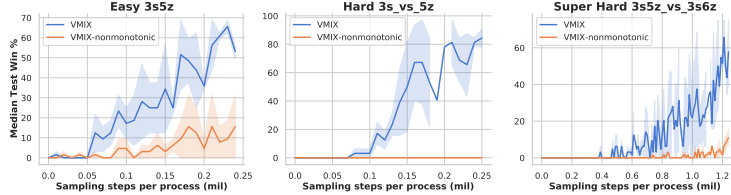


Figure 6: Comparing VMIX with and without monotonicity constraint on SMAC.

To explore the generality of monotonicity constraints, we extend the above experiments to VMIX [32]. VMIX adds the monotonicity constraint to the value network (not Q value networks) of A2C. (details in Appendix F.7) VMIX learns the policy of each agent by advantage-based policy gradient [21]; therefore, the monotonicity constraint is not necessary for greedy action selection either. We can evaluate the effects of the monotonicity constraint by removing the absolute value operation in Figure 11. The result from Figure 6 shows that the monotonicity constraint improves the sample efficiency in value networks. The above experimental results indicate that the monotonicity constraint can improve the sample efficiency in some multi-robot cooperative tasks, such as SMAC and DEPP.

## 6 Discussion

To better understand the monotonicity constraint, we discuss the following two questions with theoretical analysis. **Ques.1** Why can SMAC be represented well by monotonic mixing networks? **Ques.2** Why can the monotonicity constraint improve the sample efficiency in SMAC? To coherently answer the above questions, we give the following definitions and propositions. It is worth noting that the core assumption is that the joint action-value function  $Q_{tot}$  can be represented by a non-linear mapping  $f_{\phi}(s; Q_1, Q_2, \dots, Q_N)$ , but without the monotonicity constraint.

**Definition 1. Cooperative tasks.** For a task with  $N$  agents ( $N > 1$ ), all agents have a common goal.

**Definition 2. Semi-cooperative Tasks.** Given a cooperative task with a set of agents  $\mathbb{N}$ . For all states  $s$  of the task, if there is a subset  $\mathbb{K} \subseteq \mathbb{N}$ ,  $\mathbb{K} \neq \emptyset$ , where the  $Q_i, i \in \mathbb{K}$  increases while the other  $Q_j, j \notin \mathbb{K}$  are fixed, this will lead to an increase in  $Q_{tot}$ .

As a counterexample, the collective action problem (social dilemma) is not Semi-cooperative task. i.e., since the Q value may not include future rewards when  $\gamma < 1$ , the collective interest in the present may be detrimental to the future interest.

**Definition 3. Competitive Cases.** (Providing an example in Appendix: ??) Given two agents  $i$  and  $j$ , we say that agents  $i$  and  $j$  are competitive if either an increase in  $Q_i$  leads to a decrease in  $Q_j$  or an increase in  $Q_j$  leads to a decrease in  $Q_i$ .

**Definition 4. Purely Cooperative Tasks.** Semi-cooperative tasks without competitive cases.

As an counterexample, the matrix game as in Table 1a is not a purely cooperative task. Because of the random action sampling in reinforcement learning, we cannot guarantee that the agents share the same preferences. If one agent prefers action 0 (Like hunting) and the other agent prefers action 1 or 2 (Like sleeping or entertaining), they will have a conflict of interest (Those who like to sleep will cause the hunter to fail to catch the prey).

**Proposition 1.** Purely Cooperative Tasks can be represented by monotonic mixing networks.

*Proof.* Since the QMIX’s mixing network is a universal function approximator of monotonic functions, for a Semi cooperative task, if there is a case (state  $s$ ) that cannot be represented by a monotonic mixing network, i.e.,  $\frac{\partial Q_{tot}(s)}{\partial Q_i} < 0$ , then an increase in  $Q_i$  must lead to a decrease in  $Q_j, j \neq i$  (since there is no  $Q_j$  decrease, by Def. 2, the constraint  $\frac{\partial Q_{tot}(s)}{\partial Q_i} < 0$  does not hold). Therefore, by Def. 3 this cooperative task has a competitive case which means it is not a purely cooperative task.  $\square$

**For answering Ques.1:** According to the Proposition 1, we need to explain why SMAC is a purely cooperative task environment. SMAC mainly uses a shaped reward signal calculated from the hit-point damage dealt, some positive reward after having enemy units killed and a positive bonus for winning the battle; the reward setting can be interpreted as purely cooperative. In practice, we can decompose the hit-point damage dealt linearly and divide the units killed rewards and victory rewards to the agents near the enemy (last enemy for victory) evenly. The approximate linear decomposition<sup>5</sup> also explains why the VDNs also work well in SMAC (Table. 3).

**For answering Ques.2:** Just as in QMIX’s implementation (Figure 4) where the monotonicity constraint reduces the range of values of each mixing weight by half, the hypothesis space is assumed to decrease exponentially by  $(\frac{1}{2})^N$  ( $N$  denotes the number of weights). Note that the Q value decomposition mapping of the SMAC is a subset of the hypothesis space of QMIX’s mixing network. Therefore, using the monotonicity constraint can allow for avoiding searching invalid parameters, leading to a significant improvement in sampling efficiency.

## 7 Conclusion

In this paper, we investigate the influence of certain code-level optimizations on the performance of QMIX and provide tuning optimizations suggestions. We find that relaxing the monotonicity constraint of the mixing network will not always improve the performance of QMIX. Next, we find monotonicity constraint can improve sample efficiency in SMAC and DEPP, benefiting to the real-world robot learning. Lastly, we discuss why QMIX works well in purely cooperative tasks. Besides, we believe that the variants of QMIX that relax monotonicity constraint might be well-suited for the nonmonotonic multi-robot reinforcement learning, such as cooperative tasks with competition.

## 8 Broader Impact

Many complex real-world cooperative multi-robot problems can be simulated as CTDE multi-agent tasks. Specifically, decentralized agents can be applied to robot swarm control, vehicle coordination, and network routing. Applying MARL to these scenarios often requires a large number of samples to train the model, which implies high implementation costs, such as thousands of CPUs, power resources, and expensive robotic equipment, such as damaged drones or autonomous cars. Therefore, there is an urgent need to avoid any and all waste of such resources. In this work, the code-level optimizations and monotonicity constraint can help to improve the sample efficiency in some purely cooperative tasks, thereby reducing the wasting of resources. In addition, we focus on cooperation and competition, seen as a sort of high-level control, among multi-robots through complex computer games. Since such abstract high-level control does not require specific hardware behavior control, the gap between simulator and reality is relatively tiny. Due to the computer simulation, wasting expensive hardware can be reduced, but the characteristics of cooperation and competition can be maintained.

We believe that this work will help the community understand these approaches and drive further advances that can more quickly yield benefits for real-world applications.

---

<sup>5</sup>As  $Q_\pi(s, u) = \mathbb{E}_\pi[\sum_{k=0}^{\infty} \gamma^k r_{t+k+1} \mid s, u]$ , the reward is linearly assignable meaning that Q value is linearly assignable.

## References

- [1] M. Hüttenrauch, A. Šošić, and G. Neumann. Guided deep reinforcement learning for swarm systems. *arXiv preprint arXiv:1709.06011*, 2017.
- [2] Y. Xiao, J. Hoffman, and C. Amato. Macro-action-based deep multi-agent reinforcement learning. In *Conference on Robot Learning*, pages 1146–1161. PMLR, 2020.
- [3] O. Nachum, M. Ahn, H. Ponte, S. Gu, and V. Kumar. Multi-agent manipulation via locomotion using hierarchical sim2real. *arXiv preprint arXiv:1908.05224*, 2019.
- [4] Y. Cao, W. Yu, W. Ren, and G. Chen. An overview of recent progress in the study of distributed multi-agent coordination. *IEEE Transactions on Industrial informatics*, 9(1):427–438, 2012.
- [5] M. Zhou, J. Luo, J. Vilella, Y. Yang, D. Rusu, J. Miao, W. Zhang, M. Alban, I. Fadarar, Z. Chen, A. C. Huang, Y. Wen, K. Hassanzadeh, D. Graves, D. Chen, Z. Zhu, N. Nguyen, M. Elsayed, K. Shao, S. Ahilan, B. Zhang, J. Wu, Z. Fu, K. Rezaee, P. Yadmellat, M. Rohani, N. P. Nieves, Y. Ni, S. Banijamali, A. C. Rivers, Z. Tian, D. Palenicek, H. bou Ammar, H. Zhang, W. Liu, J. Hao, and J. Wang. Smarts: Scalable multi-agent reinforcement learning training school for autonomous driving, 2020.
- [6] C. Zhang and V. R. Lesser. Coordinated multi-agent reinforcement learning in networked distributed pomdps. In *Proceedings of the Twenty-Fifth AAAI Conference on Artificial Intelligence, AAAI 2011, San Francisco, California, USA, August 7-11, 2011*. AAAI Press, 2011.
- [7] M. Zhou, Z. Liu, P. Sui, Y. Li, and Y. Y. Chung. Learning Implicit Credit Assignment for Multi-Agent Actor-Critic. *arXiv preprint arXiv:2007.02529*, 2020.
- [8] L. Kraemer and B. Banerjee. Multi-agent reinforcement learning as a rehearsal for decentralized planning. *Neurocomputing*, 190:82–94, 2016. ISSN 09252312. doi:10.1016/j.neucom.2016.01.031.
- [9] E. Wei, D. Wicke, D. Freelan, and S. Luke. Multiagent Soft Q-Learning. *arXiv preprint arXiv:1804.09817*, 2018.
- [10] T. Rashid, M. Samvelyan, C. S. de Witt, G. Farquhar, J. N. Foerster, and S. Whiteson. QMIX: monotonic value function factorisation for deep multi-agent reinforcement learning. In *Proceedings of the 35th International Conference on Machine Learning, ICML 2018, Stockholmsmässan, Stockholm, Sweden, July 10-15, 2018*, volume 80 of *Proceedings of Machine Learning Research*, pages 4292–4301. PMLR, 2018.
- [11] J. Wang, Z. Ren, T. Liu, Y. Yu, and C. Zhang. QPLEX: Duplex Dueling Multi-Agent Q-Learning. *arXiv:2008.01062*, 2020.
- [12] Y. Yang, J. Hao, B. Liao, K. Shao, G. Chen, W. Liu, and H. Tang. Qatten: A General Framework for Cooperative Multiagent Reinforcement Learning. *arXiv preprint arXiv:2002.03939*, 2020.
- [13] T. Rashid, G. Farquhar, B. Peng, and S. Whiteson. Weighted QMIX: Expanding Monotonic Value Function Factorisation. *arXiv preprint arXiv:2006.10800*, 2020.
- [14] M. Samvelyan, T. Rashid, C. S. de Witt, G. Farquhar, N. Nardelli, T. G. J. Rudner, C.-M. Hung, P. H. S. Torr, J. Foerster, and S. Whiteson. The StarCraft Multi-Agent Challenge. *arXiv preprint arXiv:1902.04043*, 2019.
- [15] W. Boehmer, V. Kurin, and S. Whiteson. Deep coordination graphs. In *Proceedings of the 37th International Conference on Machine Learning, ICML 2020, 13-18 July 2020, Virtual Event*, volume 119 of *Proceedings of Machine Learning Research*, pages 980–991. PMLR, 2020.
- [16] B. Peng, T. Rashid, C. A. Schroeder de Witt, P.-A. Kamienny, P. H. Torr, W. Böhmer, and S. Whiteson. Facmac: Factored multi-agent centralised policy gradients. *arXiv e-prints*, pages arXiv–2003, 2020.

- [17] K. Son, D. Kim, W. J. Kang, D. Hostallero, and Y. Yi. QTRAN: learning to factorize with transformation for cooperative multi-agent reinforcement learning. In *Proceedings of the 36th International Conference on Machine Learning, ICML 2019, 9-15 June 2019, Long Beach, California, USA*, volume 97 of *Proceedings of Machine Learning Research*, pages 5887–5896. PMLR, 2019.
- [18] K. Son, S. Ahn, R. D. Reyes, J. Shin, and Y. Yi. QTRAN++: Improved Value Transformation for Cooperative Multi-Agent Reinforcement Learning. *arXiv:2006.12010*, 2020.
- [19] S. C. Ong, S. W. Png, D. Hsu, and W. S. Lee. Pomdps for robotic tasks with mixed observability. 5:4, 2009.
- [20] A. Mahajan, T. Rashid, M. Samvelyan, and S. Whiteson. MAVEN: multi-agent variational exploration. In *Advances in Neural Information Processing Systems 32: Annual Conference on Neural Information Processing Systems 2019, NeurIPS 2019, December 8-14, 2019, Vancouver, BC, Canada*, pages 7611–7622, 2019.
- [21] V. Mnih, A. P. Badia, M. Mirza, A. Graves, T. P. Lillicrap, T. Harley, D. Silver, and K. Kavukcuoglu. Asynchronous methods for deep reinforcement learning. In *Proceedings of the 33rd International Conference on Machine Learning, ICML 2016, New York City, NY, USA, June 19-24, 2016*, volume 48 of *JMLR Workshop and Conference Proceedings*, pages 1928–1937. JMLR.org, 2016.
- [22] P. Sunehag, G. Lever, A. Grusl, W. M. Czarnecki, V. Zambaldi, M. Jaderberg, M. Lanctot, N. Sonnerat, J. Z. Leibo, K. Tuyls, and T. Graepel. Value-Decomposition Networks For Cooperative Multi-Agent Learning. *arXiv preprint arXiv:1706.05296*, 2017.
- [23] J. Su, S. Adams, and P. A. Beling. Value-decomposition multi-agent actor-critics. *arXiv preprint arXiv:2007.12306*, 2020.
- [24] A. Stooke and P. Abbeel. Accelerated methods for deep reinforcement learning. *arXiv preprint arXiv:1803.02811*, 2018.
- [25] Y. Wang, B. Han, T. Wang, H. Dong, and C. Zhang. Off-Policy Multi-Agent Decomposed Policy Gradients. *arXiv:2007.12322*, 2020.
- [26] J. N. Foerster, G. Farquhar, T. Afouras, N. Nardelli, and S. Whiteson. Counterfactual multi-agent policy gradients. In *Proceedings of the Thirty-Second AAAI Conference on Artificial Intelligence, (AAAI-18), the 30th innovative Applications of Artificial Intelligence (IAAI-18), and the 8th AAAI Symposium on Educational Advances in Artificial Intelligence (EAAI-18), New Orleans, Louisiana, USA, February 2-7, 2018*, pages 2974–2982. AAAI Press, 2018.
- [27] R. Lowe, Y. Wu, A. Tamar, J. Harb, P. Abbeel, and I. Mordatch. Multi-agent actor-critic for mixed cooperative-competitive environments. In *Advances in Neural Information Processing Systems 30: Annual Conference on Neural Information Processing Systems 2017, December 4-9, 2017, Long Beach, CA, USA*, pages 6379–6390, 2017.
- [28] D. P. Kingma and J. Ba. Adam: A method for stochastic optimization. In *3rd International Conference on Learning Representations, ICLR 2015, San Diego, CA, USA, May 7-9, 2015, Conference Track Proceedings*, 2015.
- [29] R. S. Sutton and A. G. Barto. *Reinforcement learning: An introduction*. MIT press, 2018.
- [30] J. Peng and R. J. Williams. Incremental multi-step q-learning. In *Machine Learning Proceedings 1994*, pages 226–232. Elsevier, 1994.
- [31] D. Precup, R. S. Sutton, and S. P. Singh. Eligibility traces for off-policy policy evaluation. In *Proceedings of the Seventeenth International Conference on Machine Learning (ICML 2000), Stanford University, Stanford, CA, USA, June 29 - July 2, 2000*, pages 759–766. Morgan Kaufmann, 2000.
- [32] J. Su, S. Adams, and P. A. Beling. Value-Decomposition Multi-Agent Actor-Critics. *arXiv:2007.12306*, 2020.

- [33] L. Engstrom, A. Ilyas, S. Santurkar, D. Tsipras, F. Janoos, L. Rudolph, and A. Madry. Implementation Matters in Deep Policy Gradients: A Case Study on PPO and TRPO. *arXiv:2005.12729*, 2020.
- [34] J. Schulman, F. Wolski, P. Dhariwal, A. Radford, and O. Klimov. Proximal policy optimization algorithms. *arXiv preprint arXiv:1707.06347*, 2017.
- [35] M. Andrychowicz, A. Raichuk, P. Stańczyk, M. Orsini, S. Girgin, R. Marinier, L. Hussenot, M. Geist, O. Pietquin, M. Michalski, S. Gelly, and O. Bachem. What Matters In On-Policy Reinforcement Learning? A Large-Scale Empirical Study. *arXiv:2006.05990*, 2020.
- [36] T. Kozuno, Y. Tang, M. Rowland, R. Munos, S. Kapturowski, W. Dabney, M. Valko, and D. Abel. Revisiting peng’s  $q(\lambda)$  for modern reinforcement learning. *arXiv preprint arXiv:2103.00107*, 2021.
- [37] K. Cobbe, J. Hilton, O. Klimov, and J. Schulman. Phasic policy gradient. *arXiv preprint arXiv:2009.04416*, 2020.
- [38] M. Tan. Multi-agent reinforcement learning: Independent vs. cooperative agents. In *Proceedings of the tenth international conference on machine learning*, pages 330–337, 1993.
- [39] V. Mnih, K. Kavukcuoglu, D. Silver, A. Graves, I. Antonoglou, D. Wierstra, and M. Riedmiller. Playing atari with deep reinforcement learning. *arXiv preprint arXiv:1312.5602*, 2013.
- [40] Z. Wang, T. Schaul, M. Hessel, H. van Hasselt, M. Lanctot, and N. de Freitas. Dueling network architectures for deep reinforcement learning. In *Proceedings of the 33rd International Conference on Machine Learning, ICML 2016, New York City, NY, USA, June 19-24, 2016*, volume 48 of *JMLR Workshop and Conference Proceedings*, pages 1995–2003. JMLR.org, 2016.

## A Rethinking the Code-level Optimizations (Extension of Sec. 5.1)

Engstrom *et.al* [33] investigates code-level optimizations based on PPO [34] implementation, and concludes that the majority of performance differences between PPO and TRPO originate from code-level optimizations. Andrychowicz *et. al* [35] investigates the influence of code-level optimizations on the performance of PPO and provides tuning optimizations. These optimizations include: (1) Adam and Learning rate annealing. (2) Orthogonal initialization and Layer scaling. (3) Observation normalization. (4) Value normalization. (5) N-step returns (eligibility traces). (6) Reward scaling. (7) Reward clipping. Using a subset of the whole code-level optimizations, specifically shown in Sec. 5.1, we enabled QMIX to solve almost all scenarios of SMAC.

We also propose a simple trick, i.e, rewards shaping, to help QMIX learning in a non-monotonic environment.

### A.1 Rewards Shaping

**Study description.** Table 1a shows a non-monotonic case that QMIX cannot solve. However, the reward function in MARL is defined by the user; we investigate whether QMIX can learn a correct argmax action by reshaping the task’s reward function without changing its goal.

<b>12.0</b>	-0.5	-0.5
-0.5	0	0
-0.5	0	0

(a) Reshaped Payoff matrix

<b>12.0</b>	-0.3	-0.3
-0.3	-0.3	-0.3
-0.3	-0.3	-0.3

(b) QMIX:  $Q_{tot}$

Table 4: A non-monotonic matrix game in which we reshape the reward by replacing the insignificant reward -12 (in Table 1a) with reward -0.5. QMIX learns a  $Q_{tot}$  which has a correct argmax. Bold text indicates argmax action’s reward.

**Interpretation.** The reward -12 in Table 1a does not assist the agents in finding the optimal solution; as shown in Table 4, this non-monotonic matrix may be solved by simply replacing the insignificant reward -12 with -0.5. The reward shaping may also help QMIX learn more effectively in other non-monotonic tasks.

**Recommendation.** Increase the scale of the important rewards of the tasks and reduce the scale of rewards that may cause disruption.

## B Peng’s $Q(\lambda)$

TD( $\lambda$ ) can be expressed as Eq. 5:

$$G_s^\lambda \doteq (1 - \lambda) \sum_{n=1}^{\infty} \lambda^{n-1} G_{s:s+n} \tag{5}$$

$$G_{s:s+n} \doteq \sum_{t=s}^{s+n} \gamma^{t-s} r_t + \gamma^{n+1} V(s_{s+n+1}, u)$$

Peng’s  $Q(\lambda)$  replaces the V value of the next state with the max Q value, as shown in Eq. 6:

$$G_{s:s+n} \doteq \sum_{t=s}^{s+n} \gamma^{t-s} r_t + \gamma^{n+1} \max_u Q(s_{s+n+1}, u) \tag{6}$$

where  $\lambda$  is the discount factor of the traces and  $\left(\prod_{s=1}^t \lambda\right) = 1$  when  $t = 0$ . When  $\lambda$  is set to 0, it is equivalent to 1-step bootstrap returns. When  $\lambda$  is set to 1, it is equivalent to Monte Carlo [29] returns.

[36] show that while Peng’s  $Q(\lambda)$  does not learn optimal policies under arbitrary behavior policies, a convergence guarantee can be recovered if the behavior policy tracks the target policy, as is often the case in practice.

## C Predator-Prey

In the vanilla Predator-Prey [27], three cooperating agents control three robot predators to chase a faster robot prey (the preys acts randomly) by controlling their velocities with actions [up, down, left, right, stop] within an area containing two large obstacles at random locations. The goal is to capture the prey with the fewest steps possible.

**Predator-Prey** By contrast, we use a variant of Predator-Prey from [15], which requires two predators to catch the prey at the same time to get a reward. Therefore, the variant requires effective agent coordination. However, [15] added a penalty to the agents if only one predator catches the prey (not two predators at the same time), which makes the environments somewhat competitive. The penalty requires two predators capture the prey at the same time. If a diligent predator prefers to capture the prey and the other lazy one does not<sup>6</sup>, then they have conflicting interests. In our experiments, we remove the penalty to ensure that the environment is purely cooperative.

**Continuous Predator-Prey** We also use the Continuous Predator-Prey from [16]. To obtain a hard cooperative environment, [16] replaces the prey’s policy with a hard-coded heuristic that, at any time step, moves the prey to the sampled position with the largest distance to the closest predator. Therefore, the Continuous Predator-Prey is more difficult than the Predator-prey used by MADDPG [27].

## D Experimental Details

### D.1 Hyperparameters

Algorithms	Value-based (VB)	Policy-based (PG)
Optimizer	Adam, RMSProp	Adam, RMSProp
Learning Rates	0.0005, 0.001	0.0001 (for DOP), 0.0005, 0.001,
Batch Size(episode)	32, 64, 128	32, 64
Replay Buffer Size	5000, 10000, 20000	2000, 5000, 10000, 20000
$Q(\lambda)$ , $TD(\lambda)$	0, 0.3, 0.6, 0.9	0, 0.3, 0.6, 0.9
Adaptive Entropy	-	0.01, 0.03, 0.06, (add 0.0005, 0.0001, 0.001 for DOP)
$\epsilon$ Anneal Steps	50K, 100K, 500K, 1000K	-

Table 5: Hyperparameters Search on 5m\_vs\_6m and 3s5z\_vs\_3s6z.

As shown in Table 5, we perform grid search schemes on a typical hard environment (5m\_vs\_6m) and super hard environment (3s5z\_vs\_3s6z) to find a **general** set of hyperparameters for each algorithm. The reason why we avoid careful tuning of the hyperparameters for all scenarios is that robustness is also important for MARL algorithms. It is worth stating that our hyperparameter search scope contains whether to use a trick, e.g. setting  $\lambda$  to 0 is equivalent to the 1-step TD algorithm.

Based on the results of the grid search, we further explain how these hyperparameters are set. Table 6a and 6b shows our general settings for the these algorithms. The network size is calculated under 6h\_vs\_8z, where adding *Our* denotes the new hyperparameter settings.

**Neural Network Size** We first ensure the network size is the same order of magnitude, which means that we decrease the critic-net size of LICA from 29696K to 208K, and we use 4 attention heads leading the mixing-net size of QPLEX from 476K to 152K. All the agent networks are the same as those found in QMIX [10].

**Optimizer & Learning Rate** We use Adam to optimize all networks as it may accelerate the convergence of the algorithms. Furthermore, we use different learning rates for each algorithm: (1) For all value-based algorithms, neural networks are trained with 0.001 learning rate. (2) For LICA,

<sup>6</sup>Because of the random sampling in reinforcement learning, some samples with penalized rewards can cause certain agents to tend to be lazy.

Algorithms	LICA	<b>OurLICA</b>	DOP	<b>OurDOP</b>	RIIT
Optimizer	Adam	<b>Adam</b>	RMSProp	<b>Adam</b>	Adam
Batch Size(episodes)	32	32	Off=32, On=16	<b>Off=64, On=32</b>	Off=64, On=32
TD( $\lambda$ )	0.8	<b>0.6</b>	0.8, TB( $\lambda=0.93$ )	<b>0.6, TB(<math>\lambda=0.9</math>)</b>	0.6
Adaptive Entropy	0.06	0.06	-	<b>0.0005</b>	0.03
$\epsilon$ Anneal Steps	-	-	500K	-	-
Critic-Net Size	29696K	<b>208K</b>	122K	122K	69K
Rollout Processes	32	<b>8</b>	4	<b>8</b>	8

(a) Setting of Policy-based algorithms.

Algorithms	QMIX	<b>OurQMIX</b>	Qatten	<b>OurQatten</b>	QPLEX	<b>OurQPLEX</b>
Optimizer	RMSProp	<b>Adam</b>	RMSProp	<b>Adam</b>	RMSProp	<b>Adam</b>
Batch Size (epi.)	128	<b>128</b>	32	<b>128</b>	32	<b>128</b>
Q( $\lambda$ )	0	<b>0.6</b>	0	<b>0.6</b>	0	<b>0.6</b>
Attention Heads	-	-	4	4	10	<b>4</b>
Mixing-Net Size	41K	41K	58K	58K	476K	<b>152K</b>
$\epsilon$ Anneal Steps	-	50K $\rightarrow$ <b>500K for <math>6h\_vs\_8z</math>, 100 K for others</b>	-	-	-	-
Rollout Processes	8	<b>8</b>	1	<b>8</b>	1	<b>8</b>

(b) Setting of Value-based algorithm.

Table 6: Hyperparameters Settings.

we set the learning rate of the agent network to 0.0025 and the critic network’s learning rate to 0.0005. (3) For DOP, we set the agent network’s learning rate to 0.0005 and the learning rate of the critic network to 0.0001. (4) For RIIT, we set the learning rates to 0.001.

**Batch Size** We find that a large batch size helps to improve the stability of the algorithms. Therefore, for value-based algorithms, we set the batch size to 128. For the policy-based algorithms, we set the batch size to 64/32 (Offline/Online training) due to the fact that online sample requires only the newest data.

**Replay Buffer Size** As discussed in Sec. 5.1.3, a small replay buffer size facilitates the convergence of the MARL algorithms. Therefore, for SMAC, the size of all replay buffers is set to 5000 episodes. For Predator-Prey, we set the buffer size to 1000 episodes.

**Exploration** As discussed in Sec. 5.1.5, we use  $\epsilon$ -greedy action selection, decreasing  $\epsilon$  from 1 to 0.05 over n-time steps (n can be found in Table 6b) for value-based algorithms. We use the Adaptive Entropy (Appendix. F.6) for all policy-based algorithms because it facilitates the automatic adjustment of the size of the entropy loss in different scenarios. We also add the Adaptive Entropy to DOP to prevent it from crashing.

**Q( $\lambda$ )** Since replay buffer size and  $\epsilon$  are set to small values, the convergence of Q( $\lambda$ ) is guaranteed. We find that the value of Q( $\lambda$ ) is closely related to the test scenarios. We are using  $\lambda = 0.6$  for all tasks as the value works stably in most scenarios.

**Rollout Processes Number** Eight rollout processes for parallel sampling are used to obtain as many samples as possible from the environments at a high rate. This also ensures that all the algorithms share the same number of policy iterations and sample size (10 million).

**Other Settings** We set all discount factors  $\gamma = 0.99$ . We update the target network every 200 episodes. We do not reshape the reward of SMAC and Predator-Prey, as they provide a default shaping reward. We find that the optimal hyperparameters of the value-based algorithms are similar due to the fact that they share the same basic architecture and training paradigm. Therefore, the settings for VDNs and WQMIX are the same as for QMIX. Specifically, we use OW-QMIX, detailed in F.5, in WQMIX as the baseline. Note that our experimental results are not directly comparable with the previous works (which use SC2.4.6), as we use StarCraft 2 (SC2.4.10) in the latest PyMARL.

## D.2 Omitted Experimental Results

We echo our experiments in Sec. 5.2.1. Figure 7 and 8 shows that QMIX achieves excellent performance on all hard scenarios in SMAC, and outperforms other algorithms. Figure 8 shows that

QPLEX’s policy collapses in the test of Super Hard *6h\_vs\_8z* and *corridor*<sup>7</sup>. Figure 9 shows that each of the algorithms achieves good performance on DEPP. The win rates in Figure 8 are lower than in Table 3 as we smoothed these curves.

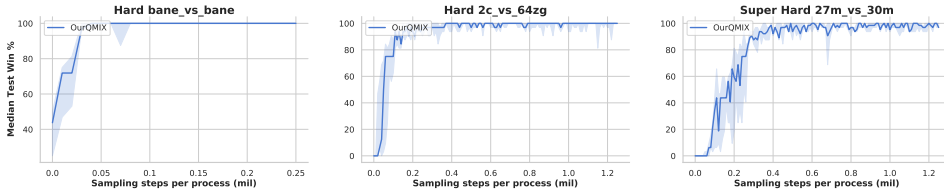


Figure 7: Median test win rate of OurQMIX on Hard Scenarios in SMAC.

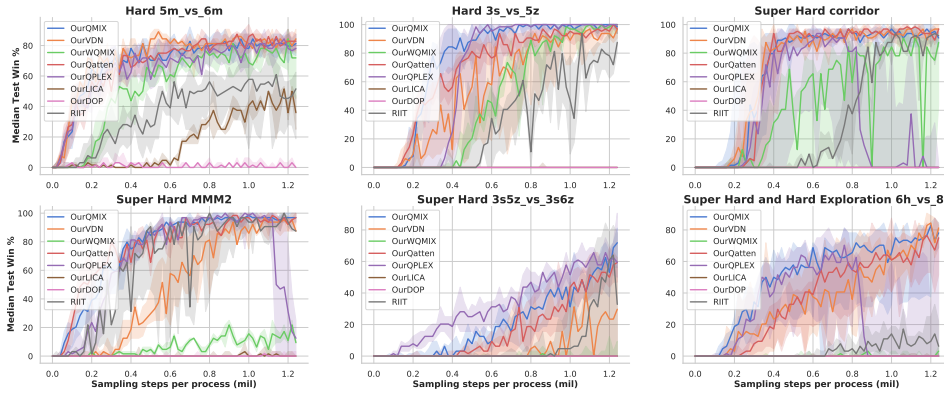


Figure 8: Median test win rate of MARL algorithms on SMAC.

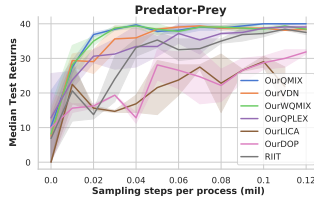


Figure 9: Median episode return of MARL algorithms on Predator-Prey.

### D.3 Comparing with Original Algorithm

In this section, we make a simple horizontal comparison for the original algorithms. We compare their original performance with third-party experimental results, i.e. experimental results of the paper citing the algorithm.

For VDNs and QMIX, the original SMAC paper [14] shows that VDNs and QMIX do not perform well in hard and super hard scenarios. For Qatten, the experiments in [11] demonstrates that the performance of Qatten is worse than vanilla QMIX. [16] demonstrates that QPLEX and DOP does not work well in hard and super hard scenarios in SMAC, and the their performance is worse than vanilla QMIX. It is interesting that WQMIX [13] shows the poor performance of WQMIX in super hard scenarios *3s5z\_vs\_3s6z* and *corridor*. The original test results in LICA are not considered as 64 million samples are used in their experiments.

However, after our hyperparameter tuning, all the value-based methods achieve good performance in Hard and Super Hard scenarios. Therefore, *Our* method, i.e. OurVDNs, OurQatten, OurQPELX, OurWQMIX have better performance than the original ones.

<sup>7</sup>It may be that QPLEX feeds both actions and states into the mixing network in its implementation. The mixing network can predict true  $Q_{tot}$  without correct  $Q_i$ , so that the  $Q_i$  becomes useless.

## E RIIT

RIIT decomposes training into offline and online phases; we use offline samples to train the critic network with 1-step TD error loss; then, we use the online samples to train policy networks end-to-end and critic with TD( $\lambda$ ). Training policy networks with online samples improve learning stability<sup>8</sup>. Furthermore, the offline training phase improves sample efficiency for critic networks. Algo. 1 demonstrates the training process of RIIT.

---

### Algorithm 1 Optimization Procedure for RIIT

---

Initialize offline replay memory  $D$  and online replay memory  $D'$ .

Randomly initialize  $\theta$  and  $\phi$  for the policy networks and the mixing critic respectively.

Set  $\phi^- \leftarrow \phi$ .

**while** not terminated **do**

  # Off-policy stage

  Sample  $b$  episodes  $\tau_1, \dots, \tau_b$  with  $\tau_i = \{s_{0,i}, o_{0,i}, u_{0,i}, r_{0,i}, \dots, s_{T,i}, o_{T,i}, u_{T,i}, r_{T,i}\}$  from offline replay memory  $D$ .

  Update the monotonic mixing network with  $y_{t,i}$  calculated by 1-step bootstrap return ( $y_{t,i} = r_{t,i} + \gamma Q_{\phi^-}^\pi(s_{t+1}, \vec{u}_{t+1})$ ):

$$\nabla_{\phi} \frac{1}{bT} \sum_{i=1}^b \sum_{t=1}^T (y_{t,i} - Q_{\phi}^\pi(s_{t,i}, u_{t,i}^1, \dots, u_{t,i}^n))^2. \quad (7)$$

  # On-policy stage

  Sample  $b$  episodes  $\tau_1, \dots, \tau_b$  with  $\tau_i = \{s_{0,i}, o_{0,i}, u_{0,i}, r_{0,i}, \dots, s_{T,i}, o_{T,i}, u_{T,i}, r_{T,i}\}$  from online replay memory  $D'$ .

  Update the monotonic mixing network with  $y_{t,i}^{TD(\lambda)}$  calculated by TD( $\lambda$ ) (Eq. 5):

$$\nabla_{\phi} \frac{1}{bT} \sum_{i=1}^b \sum_{t=1}^T (y_{t,i}^{TD(\lambda)} - Q_{\phi}^\pi(s_{t,i}, u_{t,i}^1, \dots, u_{t,i}^n))^2. \quad (8)$$

  Update the decentralized policy networks end-to-end by maximizing the Q value, with adaptive entropy loss (Appendix F.6):

$$\nabla_{\theta} \frac{1}{bT} \sum_{i=1}^b \sum_{t=1}^T \left( Q_{\phi}^\pi(s_{t,i}, \pi_{\theta_1}^1(\cdot|z_{t,i}^1), \dots, \pi_{\theta_n}^n(\cdot|z_{t,i}^n)) + \frac{1}{n} \sum_{a=1}^n \mathcal{H}(\pi_{\theta_a}^a(\cdot|z_{t,i}^a)) \right). \quad (9)$$

**if** at target update interval **then**

    Update the target mixing network  $\phi^- \leftarrow \phi$ .

**end if**

**end while**

---

<sup>8</sup>[37] shows that actor networks generally have a lower tolerance for sample reuse than critic networks

## F Cooperative MARL

### F.1 IQL

Independent Q-learning (IQL) [38] breaks down a multi-agent task into a series of simultaneous single-agent tasks that share the same environment, just like multi-agent Deep Q-networks (DQN) [39]. DQN represents the action-value function with a deep neural network parameterized by  $\theta$ . DQN uses a replay buffer to store transition tuple  $(s, u, r, s')$ , where state  $s'$  is observed after taking action  $u$  in state  $s$  and obtaining reward  $r$ . However, IQL does not address the non-stationarity introduced due to the changing policies of the learning agents. Thus, unlike single-agent DQN, there is no guarantee of convergence even at the limit of infinite exploration.

### F.2 VDNs

By contrast, Value decomposition networks (VDNs)<sup>9</sup> [22] seek to learn a joint action-value function  $Q_{tot}(\boldsymbol{\tau}, \mathbf{u})$ , where  $\boldsymbol{\tau} \in \mathbf{T} \equiv \mathcal{T}^n$  is a joint action-observation history and  $\mathbf{u}$  is a joint action. It represents  $Q_{tot}$  as the sum of individual value functions  $Q_a(\tau^i, u^i; \theta^i)$ :

$$Q_{tot}(\boldsymbol{\tau}, \mathbf{u}) = \sum_{i=1}^n Q_i(\tau^i, u^i; \theta^i).$$

### F.3 Qatten

**Qatten**<sup>10</sup> [12], introduces an attention mechanism into the monotonic mixing network of QMIX:

$$Q_{tot} \approx c(s) + \sum_{h=1}^H w_h \sum_{i=1}^N \lambda_{i,h} Q^i \quad (10)$$

$$\lambda_{i,h} \propto \exp(e_i^T W_{k,h}^T W_{q,h} e_s) \quad (11)$$

where  $w_h = |f^{NN}(s)|_h$ ,  $W_{q,h}$  transforms  $e_s$  into a global query, and  $W_{k,h}$  transforms  $e_i$  into an individual key. The  $e_s$  and  $e_i$  may be obtained by an embedding transformation layer for the true global state  $s$  and the individual state  $s_i$ .

### F.4 QPLEX

**QPLEX**<sup>11</sup> [11] decomposes Q values into advantages and values based on Qatten, similar to Dueling-DQN [40]:

$$\begin{aligned} \text{(Joint Dueling)} \quad Q_{tot}(\boldsymbol{\tau}, \mathbf{u}) &= V_{tot}(\boldsymbol{\tau}) + A_{tot}(\boldsymbol{\tau}, \mathbf{u}) \\ V_{tot}(\boldsymbol{\tau}) &= \max_{u'} Q_{tot}(\boldsymbol{\tau}, u') \end{aligned} \quad (12)$$

$$\begin{aligned} \text{(Individual Dueling)} \quad Q_i(\tau_i, u_i) &= V_i(\tau_i) + A_i(\tau_i, u_i) \\ V_i(\tau_i) &= \max_{u'} Q_i(\tau_i, u') \end{aligned} \quad (13)$$

$$\frac{\partial A_{tot}(s, \mathbf{u}; \boldsymbol{\theta}, \phi)}{\partial A_i(\tau^i, u^i; \theta^i)} \geq 0, \quad \forall i \in \mathcal{N} \quad (14)$$

In other words, Eq. 14 (advantage-based monotonicity) transfers the monotonicity constraint from Q values to advantage values. QPLEX thereby reduces limitations on the mixing network's expressiveness.

<sup>9</sup>VDN code: <https://github.com/oxwhirl/pymarl>

<sup>10</sup>Qatten code: <https://github.com/simsimiSION/pymarl-algorithm-extension-via-starcraft>

<sup>11</sup>QPLEX code: <https://github.com/wjh720/QPLEX>

## F.5 WQMIX

**WQMIX**<sup>12</sup> [13], just like Optimistically-Weighted QMIX (OW-QMIX), uses different weights for each sample to calculate the squared TD error of QMIX:

$$\mathcal{L}(\theta) = \sum_{i=1}^b w(s, \mathbf{u}) (Q_{tot}(\boldsymbol{\tau}, \mathbf{u}, s) - y_i)^2 \quad (15)$$

$$w(s, \mathbf{u}) = \begin{cases} 1 & Q_{tot}(\boldsymbol{\tau}, \mathbf{u}, s) < y_i \\ \alpha & \text{otherwise.} \end{cases} \quad (16)$$

Where  $\alpha \in (0, 1]$  is a hyperparameter and  $y_i$  is the true target Q value. WQMIX prefers those optimistic samples (true returns are larger than predicted), i.e., decreasing the weights of samples with non-optimistic returns. More critically, WQMIX uses an unconstrained true Q Network as a target network to guide the learning of QMIX. The authors prove that this approach can resolve the estimation errors of QMIX in the non-monotonic case.

## F.6 LICA

**LICA**<sup>13</sup> [7] completely removes the monotonicity constraint through a policy mixing critic, as shown in Figure 10:

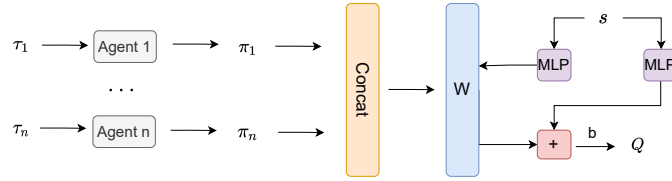


Figure 10: Architecture for LICA. LICA’s mixing critic maps policy distribution to the Q value directly, in effect obviating the monotonicity constraint.

LICA’s mixing critic is trained using squared TD error. With a trained critic estimate, decentralized policy networks may then be optimized end-to-end simultaneously by maximizing  $Q_{\theta_c}^{\pi}$  with the stochastic policies  $\pi_{\theta_i}^i$  as inputs:

$$\max_{\theta} \mathbb{E}_{t, s_t, u_t^1, \dots, \tau_t^n} [Q_{\theta_c}^{\pi}(s_t, \pi_{\theta_1}^1(\cdot | \tau_t^1), \dots, \pi_{\theta_n}^n(\cdot | \tau_t^n)) + \mathbb{E}_i [\mathcal{H}(\pi_{\theta_i}^i(\cdot | \tau_t^i))]] \quad (17)$$

where the gradient of entropy item  $\mathbb{E}_i [\mathcal{H}(\pi_{\theta_i}^i(\cdot | z_t^i))]$  is normalized by taking the quotient of its own modulus length: Adaptive Entropy (Adapt Ent). Adaptive Entropy automatically adjusts the coefficient of entropy loss in different scenarios.

## F.7 VMIX

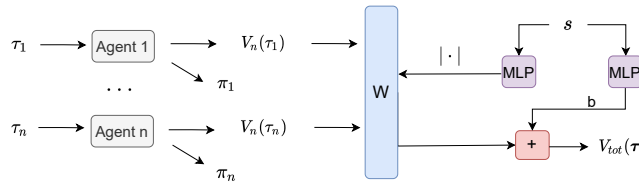


Figure 11: Architecture for VMIX:  $|\cdot|$  denotes **absolute value operation**, decomposing  $V_{tot}$  into  $V_i$ .

<sup>12</sup>WQMIX code: <https://github.com/oxwhirl/wqmix>

<sup>13</sup>LICA code: <https://github.com/mzho7212/LICA>

VMIX<sup>14</sup> [23] combines the Advantage Actor-Critic (A2C) [24] with QMIX to extend the monotonicity constraint to value networks (not Q value network), as shown in Eq. 19 and Figure 11. We verified that the monotonicity constraint also has a positive effect on the value network based on VMIX (Figure 6).

$$\begin{aligned}
 & V_{tot}(s; \boldsymbol{\theta}, \phi) \\
 & = g_{\phi}(s, V^1(\tau^1; \theta^1), \dots, V^N(\tau^N; \theta^N))
 \end{aligned} \tag{18}$$

$$\frac{\partial V_{tot}}{\partial V^i} \geq 0, \quad \forall i \in \{1, \dots, N\} \tag{19}$$

where  $\phi$  is the parameter of value mixing network, and  $\theta_i$  is the parameter of agent network. With the centralized value function  $V_{tot}$ , the policy networks can be trained by policy gradient (Eq. 20),

$$\hat{g}_i = \frac{1}{|\mathcal{D}|} \sum_{\tau \in \mathcal{D}} \sum_{t=0}^T \nabla_{\theta} \log \pi_{\theta^i}(u_t^i | \tau_t^i) \Big|_{\theta^i} \hat{A}_t \tag{20}$$

where  $\hat{A}_t = r + V_{tot}(s') - V_{tot}(s)$  is the advantage function, and  $\mathcal{D}$  denotes replay buffer.

## F.8 Relationship between Previous Works

VDNs requires a linear decomposition of Q values, so it has the strongest monotonicity constraint. Since the weights calculated by softmax (attention mechanism) are greater than or equal to zero, Qatten and QMIX share the same constraint strength. QPLEX just shifts the constraint to advantage values without removing it. WQMIX relaxes the monotonicity constraint even further by a true Q value network and theoretical guarantees. LICA completely removes the monotonicity constraint by new network architecture. We rank the strength of the monotonicity constraints on these MARL algorithms:

$$VDNs > QMIX = Qatten > QPLEX > WQMIX > LICA.$$

---

<sup>14</sup>VMIX code: <https://github.com/hahayonghuming/VDACs>